The Abundance of Seafloor Massive Sulfide Deposits

Mark Hannington[1], John Jamieson[1], Thomas Monecke[2], Sven Petersen[3], Stace Beaulieu[4]

[1]Department of Earth Sciences, University of Ottawa, Ottawa, Canada, K1N 6N5. [2]Department of Geology and Geological Engineering, Colorado School of Mines, CO 80401. [3]Leibniz Institute of Marine Sciences, IFM-Geomar, 24148 Kiel, Germany. [4]Woods Hole Oceanographic Institution, Woods Hole, MA 02543, USA.

Supplemental Information

1. Method of Analysis

The model results presented in this paper are analogous to those routinely used to assess the undiscovered mineral potential of different ore deposit types on land and follow the 3-part mineral assessment practice of the U.S. Geological Survey (Mosier et al., 2007, 2009; Singer, 2010; Singer and Menzie, 2010). The first step involves an examination of geological maps to determine the area that may be permissive for the discovery of new deposits. The second step is an estimate of the number of undiscovered deposits in that area based on the measurement of deposit densities in well-explored control areas. The third step is an estimate of the probable sizes of undiscovered mineral deposits using data from well-explored examples that are assumed to be representative of the total population. The essential criterion is that all deposits are represented by the same density and size distributions developed from examples in the control areas.

2. Global Database of Seafloor Hydrothermal Systems

Deposit occurrence data used in this paper are from a global inventory of seafloor hydrothermal systems originally compiled for the International Seabed Authority in 2002, and updated in 2004 and 2009 (Hannington et al., 2002; 2004; Hannington and Monecke, 2009). An on-line database derived in large part from these compilations is now maintained by InterRidge

(InterRidge Vents Database, http://www.interridge.org/IRvents/: Beaulieu, 2010). The database contains information on the latitude and longitude, water depth, types of hydrothermal activity, site descriptions, deposit descriptions and related occurrences of seafloor hydrothermal activity or indications of mineralization for all parts of the ocean. Version 2.0 of the database includes 554 listings as of 5 March, 2010. The listings are comprehensive for active vent sites and also include a number of inferred active sites (unconfirmed) from separate but overlapping datasets of plumes compiled for the NOAA Vents Program (E. Baker). The main part of the database used in this study is a listing of known sulfide occurrences from M. Hannington, S. Petersen and T. Monecke (Hannington et al., 2002; 2004; Hannington and Monecke, 2009). An additional 92 vent fields were added from the literature and cruise reports through the end of 2009 by S. Beaulieu. An interactive map of these data is available for download and display in Google Earth© from InterRidge (vents_interridge_2009_all.kml).

A subset of data from 165 sites known to host discrete massive sulfide deposits was analyzed in this study (**Figure DR1** and **Table DR1**). In the analysis, a sulfide occurrence is defined as any discrete body of polymetallic massive sulfide (e.g., chimney complex or mound), commonly but not necessarily associated with active hydrothermal venting, or a cluster of such bodies within a defined area that is spatially separated from the next nearest cluster. When an occurrence consists of more than one sulfide body (e.g., a collection of chimneys or mounds), some degree of continuity is implied in order to avoid counting individual vents or chimneys as "deposits".

3. Selection of Control Areas and Measurement of Deposit Densities

Deposit densities in different parts of the oceans were determined from well-explored areas with known occurrences, chosen to represent similarly permissive areas that have not yet been explored. 32 control areas were chosen in this study, containing 129 sulfide occurrences (**Figure DR2**); 106 individual deposits or clusters of deposits more than 10 km apart were used in the measurement of deposit densities. The number of control areas chosen is similar to the number of control areas used in land-based mineral assessments (Mosier et al., 2007). Each area was of roughly equal size (5° of latitude x 5° of longitude), measuring approximately 500 km on

each side (~300,000 km^2) and containing at least 2 deposits. The map scale (1:2,500,000) was chosen so that the quality of map data was the same in all cases. This corresponds to the smallest map scale recommended for such assessments on land (Mosier et al., 2007).

On each map, a 0.1 degree grid was overlain on the areas considered to be permissive for seafloor massive sulfide occurrences, +/- 50 km from the axis of the neovolcanic zone. Defined in this way, the total area of permissive geology in each control area was close to 50,000 km^2. The placement of the grid was based on a number of different geological criteria (e.g., coverage of the ridge axis, off-axis seamounts, overlapping spreading centers, etc.). In some cases the permissive area is large, due to the presence of more than one major geologic feature of interest (e.g., areas with multiple ridge segments or overlapping spreading centers such as the Easter Microplate). Bathymetric data used to define permissive areas were derived from the GEBCO 1-minute gridded digital atlas of the seafloor (British Oceanographic Data Center, 2003). The standard GEBCO contour interval, 500 m, was used here. The maps were originally plotted as equidistant cylindrical projections allowing direct measurement of permissive areas and spacings between deposits (Hannington and Monecke, 2009). The same data may now be derived directly from the interactive map of vent sites available from InterRidge and from the Global Multi-resolution Topography Synthesis GeoMapApp (Ryan et al., 2009) Marine Geoscience Data System (MGDS) hosted by the Lamont-Doherty Observatory at Columbia University (http://www.geomapapp.org). The InterRidge vents database Version 2.0 is available in the GeoMapApp synthesis.

In the 32 controls areas selected for analysis, sufficient exploration has been carried out to be reasonably assured that a high proportion of the largest deposits have been discovered. However, an important assumption in the application of data from the control areas is that all of the deposits are known and that the current inventory will not change significantly with further exploration in those areas. Clearly, the numbers of deposits will be underestimated if the control areas have not been adequately explored. In this first order assessment, no attempt was made to rank the control areas in terms of the quality and quantity of mapping; all were assumed to have been equally explored. A number of locations with known seafloor massive sulfide occurrences were not included as control areas owing to a lack of exploration. These include, in particular,

the areas of the Arctic Ridges where only a few deposits have so far been located (e.g., Kolbeinsey Ridge, Mohns Ridge, Gakkel Ridge).

The average area of permissive geology in all 32 control areas was 54,000 km^2, although this ranged from 110,000 km^2 to as little as 25,000 km^2. Deposit densities for each control area were determined from the size of the permissive area and the number of deposits in the area (90% of the controls have densities of 2 or more deposits per 100,000 km^2, 50% have densities of 6 or more deposits, and 10% have densities of 10 or more deposits per 100,000 km^2). Deposit densities in the neovolcanic zone were also determined simply by dividing the number of known deposits by the ridge or arc length in the control area and by measuring the distances between adjacent deposits. The latter approach, used in this paper, is considered more reliable as it allows that additional discoveries may be made within the control areas beyond the known deposits.

Because of the scale of the maps used, the deposits were grouped so that the spacing between sulfide occurrences was always larger than the maximum dimension of the largest vent field. For example, on the Juan de Fuca Ridge, eight vent complexes that occur over a strike length of 10 km in the Endeavour Vent Field were grouped as one deposit; the next nearest deposit (Middle Valley) is 60 km away. We did not distinguish between deposits that consists of a cluster of vent complexes, such as the Endeavour Field, and a cluster of larger mounds in the same-sized area (e.g., the TAG, MIR, and Alvin zones in the TAG Hydrothermal Field on the Mid-Atlantic Ridge). Both are considered single deposits. Distances greater than 333 km (corresponding to the maximum L value of Baker, 2007) were considered to be out of range.

To estimate the total numbers of deposits in the neovolcanic zones, the simplest definition of the permissive "area" was used, corresponding to the cumulative strike length of the oceanic plate boundaries (89,000 km), together with the average spacing between deposits on the ridges, arcs, and back-arc spreading centers (107 km). For the mid-ocean ridges, a comparison of deposit spacing versus spreading rate (**Figure DR3**) clearly shows that the deposits are not uniformly distributed and the space between deposits increases linearly with decreasing spreading rate, as predicted by heat flux (Baker, 2007) and plume data (Baker and German, 2004; Baker et al., 2004). Thus, the number of deposits on the slow-spreading ridges may be as

much as a factor of 2 lower than estimated from a uniform deposit spacing, and the number of deposits on the fast-spreading ridges a factor of 2 higher. However, any effect on the cumulative tonnage of massive sulfide is likely offset by the large differences in the sizes of the deposits on fast and slow ridges (see below). The expected number of deposits estimated from the spacing between individual deposits is also slightly larger than that estimated from the total permissive area in each map, confirming that there is a degree of clustering at the scale of the maps used. The plume data provide important constraints on the possible numbers of seafloor massive sulfide deposits; however, physical or chemical evidence of a buoyant plume above a vent field is not necessarily an indication that significant accumulation of sulfide has occurred at the seafloor. Inactive deposits also are not captured in the plume data. Thus, the database of both active and inactive deposits studied here is considered to provide a more reliable record of metal accumulation.

4. Deposit Sizes

Once an estimate has been made of the number of deposits, it is possible to place some constraints on the amount of undiscovered massive sulfide by assuming a mass distribution similar to that of the known deposits. Only first-order estimates of deposit sizes are possible because most are incompletely mapped. The widespread dusting of metalliferous sediment and debris from collapsed chimneys makes it difficult to assess the continuity of sulfide bodies even with the most sophisticated survey techniques. **Table DR1** includes information on deposit sizes for a subset of 62 of the best documented sulfide occurrences in the database.

42 of the deposits in **Table DR1** are considered to have outcrop dimensions on the seafloor of at least 100 m^2. Using the area versus tonnage relationship for some of the best documented examples (e.g., 2.1 million tonnes in a chimney zone covering 90,000 m^2 at Solwara 1), tonnages were assigned to each deposit larger than 100 m^2 based on the measured surface area of sulfide outcrop. This assumes that all deposits have a uniform thickness, which is reasonable considering their broadly similar shapes. However, a range of possible sizes is assigned in most cases because of the large uncertainties in the areas of sulfide outcrop. The tonnages of three of the largest deposits have been confirmed by drilling (i.e., TAG, Middle

Valley, and Solwara 1: Hannington et al., 1998; Zierenberg et al., 1998; Lipton, 2008); several others have outcrop dimensions that are consistent with a total amount of massive sulfide exceeding 2 million tonnes (e.g., Sunrise, Krasnov, Semyenov, Puy des Folles, and Zenith-Victory) (Iizasa et al., 1999; Beltenev et al., 2007; Cherkashov et al., 2010). Fewer than 1 in 10 deposits are considered to be this large; the remainder of the deposits were classified into "bins" between 3,000 tonnes and 2 million tonnes.

We used the cumulative frequency of the size estimates of deposits listed in **Table DR1** to construct a first-order tonnage model for seafloor massive sulfide deposits (**Figure DR4**: Hannington et al., 2010). Individual deposits were plotted at the midpoints of the assigned tonnage ranges. About 33% of the deposits are considered to be no larger than 3,000 tonnes; they are included in the cumulative frequency but are not shown in the tonnage plot. Because the largest deposits typically have been the most carefully surveyed, they may be overrepresented in the data set, raising the possibility that the model will overestimate tonnages of massive sulfide on the seafloor. With additional exploration or drilling some deposits may be moved from one size class to another, but the general features of the size distribution are expected to remain the same. Because of the large numbers of small deposits included, the median deposit size is not expected to change significantly with new data. The discovery of one or more large deposits (>10 million tonnes) would increase the proportion of massive sulfide in the 10th percentile but not the median deposit size. The Atlantis II deposit is not included in the tonnage model used here because of its unique geological setting and style of mineralization (Hannington et al., 2005), which suggest that it does not belong to the population being modeled, although it was included in the measurement of deposit densities. Pooling of the data from fast and slow-spreading ridges and from the volcanic arcs and back-arc basins assumes that the deposits in all of these settings have the same size distribution. So far, no deposits have been found in back-arc basins or on active volcanic arcs that are significantly larger than those on mid-ocean ridges. Therefore, a separate tonnage model for subduction-related environments is not justified at this time. A least-squares regression of deposit density as a function of spreading rate on the mid-ocean ridges (**Figure DR3**), together with the size distribution of deposits in **Figure DR4**, provides the input for estimating the proportion of massive sulfide on mid-ocean ridges at different spreading rates (Figure 3 in the paper).

REFERENCES CITED

Baker, E.T., 2007, Hydrothermal cooling of midocean ridge axes: Do measured and modeled heat fluxes agree?: Earth and Planetary Science Letters, v. 263, p. 140-150.

Baker, E.T., and German, C.R., 2004, On the global distribution of mid-ocean ridge hydrothermal vent-fields: American Geophysical Union, Geophysical Monograph 148, p. 245-266.

Baker, E.T., Edmonds, H.N., Michael, P.J., Bach, W., Dick, H.J.B., Snow, J.E., Walker, S.L., Banerjee, N.R., and Langmuir, C.H., 2004, Hydrothermal venting in magma deserts: The ultraslow-spreading Gakkel and Southwest Indian Ridges: Geochemistry, Geophysics, and Geosystems, v. 5, doi:10.1029/2004GC000712.

Beaulieu, S.E., 2010, InterRidge Global Database of Active Submarine Hydrothermal Vent Fields, Version 2.0: http://www.interridge.org/IRvents.

Beltenev, V., Ivanov, V., Rozhdestvenskaya, I., Cherkashov, G., Stepanova, T., Shilov, V., Pertsev, A., Davydov, M., Egorov, I., Melekestseva, I., Narkevsky, E., and Ignatov, V., 2007, A new hydrothermal field at 13°30'N on the Mid-Atlantic Ridge: InterRidge News , v. 16, p. 9-10.

British Oceanographic Data Centre, 2003, General Bathymetric Charts of the Oceans GEBCO Digital Atlas: Intergovernmental Oceanographic Commission and the International Hydrographic Organization, Liverpool, UK (CD-ROM).

Cherkashov, G., Beltenev, V., Ivanov, V., Lazareva, L., Samovarov, M., Shilov, V., Stepanova, T., Glasby, G.P., and Kuznetsov, V., 2010, Seafloor massive sulfides from the northern equatorial Mid-Atlantic Ridge: New discoveries and perspectives: Marine Georesources and Geotechnology, v. 28, p. 222-239.

Hannington, M., and Monecke, T., 2009, Global exploration models for polymetallic sulphides in the Area: An assessment of lease block selection under the Draft Regulations on Prospecting and Exploration for Polymetallic Sulphides: Marine Georesources and Geotechnology, v. 27, p. 132-159.

Hannington, M.D., Galley, A.G., Herzig, P.M., and Petersen, S., 1998, Comparison of the TAG Mound and stockwork complex with Cyprus-type massive sulfide deposits, in Herzig, P.M.,

Humphris, S.E., Miller, D.J. and Zierenberg, R.A., eds., Proceedings of the Ocean Drilling Program, Scientific Results Volume 158: College Station, Texas, p. 389-415.

Hannington, M.D., de Ronde, C.E.J., and Petersen, S., 2005, Sea-floor tectonics and submarine hydrothermal systems, in Hedenquist, J.W., Thompson, J.F.H., Goldfarb, R.J., and Richards, J.P., eds., Economic Geology 100th Anniversary Volume, Society of Economic Geologists, p. 111-141.

Hannington, M.D., Jamieson, J., Monecke, T., and Petersen, S., 2010, Modern seafloor massive sulfides and base metal resources: Towards an estimate of global seafloor massive sulfide potential: Society of Economic Geologists Special Publication 15, p. 317-338.

Hannington, M.D., Petersen, S., Herzig, P.M., and Jonasson, I.R., 2002, A global database of seafloor hydrothermal systems, including a geochemical database of polymetallic sulphides: International Seabed Authority of the United Nations, Central Data Repository (http://www.isa.org.jm).

Hannington, M.D., Petersen, S., Herzig, P.M., and Jonasson, I.R., 2004, A global database of seafloor hydrothermal systems, including a digital database of geochemical analyses of seafloor polymetallic sulfides: Geological Survey of Canada Open File 4598, 1 CD-ROM.

Iizasa, K., Fiske, R.S., Ishizuka, O., Yuasa, M., Hashimoto, J., Ishibashi, J., Naka, J., Horii, Y., Fujiwara, Y., Imai, A., and Koyama, S., 1999, A Kuroko-type polymetallic sulfide deposit in a submarine silicic caldera: Science, v. 283, p. 975-977.

Lipton, I., 2008, Mineral resource estimate, Solwara 1 project, Bismarck Sea, Papua New Guinea: NI43-101 Technical Report for Nautilus Minerals Inc. (http://www.nautilusminerals.com/i/pdf/2008-02-01_Solwara1_43-101.pdf).

Mosier, D.L., Singer, D.A., and Berger, V.I., 2007, Volcanogenic massive sulfide deposit density: U.S. Geological Survey Scientific Investigations Report 2007-5082, p. 1-15.

Mosier, D.L., Berger, V.I., and Singer, D.A., 2009, Volcanogenic massive sulfide deposits of the world-database and grade and tonnage models: U.S. Geological Survey Open-File Report 2009-1034, p. 1-46.

Ryan, W.B.F., Carbotte, S.M., Coplan, J.O., O'Hara, S., Melkonian, A., Arko, R., Weissel, R.A., Ferrini, V., Goodwillie, A., Nitsche, F., Bonczkowski, J., and Zemsky, R. 2009, Global multi-resolution topography synthesis: Geochemistry, Geophysics, and Geosystems, v. 10, doi:10.1029/2008GC002332.

Singer, D.A., and Menzie, W.D., 2010, Quantitative Mineral Resource Assessments – An Integrated Approach: Oxford University Press, 232 p.

Singer, D.A., 2010, Progress in integrated quantitative mineral resource assessments: Ore Geology Reviews doi:10.1016/j.oregeorev.2010.02.001.

Zierenberg, R.A., Fouquet, Y., Miller, D.J., and Shipboard Scientific Party, 1998, The deep structure of a sea-floor hydrothermal deposit: Nature , v. 392, p. 485-488.

Figure DR1. Locations of 165 sites of seafloor massive sulfide deposits listed in **Table DR1** (filled circles, modified from Hannington et al., 2005). Other low-temperature hydrothermal vents and related mineralization are indicated by open circles. Major spreading ridges and subduction zones are also shown. A number of clusters of deposits are represented by just one symbol (e.g., Bent Hill, ODP Mound, Area of Active Venting at Middle Valley, no. 89). Summary data for 129 sites are listed in **Table DR2**.

Figure DR2. Locations of 32 control areas used to assess deposit densities. The numbers correspond to the entries in **Table DR2**. Mid-ocean ridges: (1) Northern Juan de Fuca Ridge, (2) Southern Juan de Fuca Ridge, (3) Gorda Ridge, (4) 21°N EPR, (5) 13°N EPR, (6) 9°N EPR, (7) 2°N EPR, (8) 7°S EPR, (9) 17°S EPR, (10) 18°S EPR, (11) 23°S Easter Microplate, (12) 37°S Pacific-Antarctic Ridge, (13) Galapagos Rift, (14) Guaymas Basin, (15) 37°N MAR (Lucky Strike, Menez Gwen), (16) 26°N MAR (TAG, Broken Spur), (17) 24°N MAR, (18) 14°N MAR (Logatchev), (19) 5°S MAR, (20) Central Indian Ridge, (21) Northern Red Sea, (22) Southern Red Sea. Arcs and back-arc basins: (23) Tyrrhenian Sea, (24) North-Central Okinawa Trough, (25) Southern Okinawa Trough, (26) Izu-Bonin Arc, (27) Southern Mariana Trough and Arc, (28) Eastern Manus Basin, (29) North Fiji Basin, (30) Southern Lau Basin, (31) Southern Kermadec Arc, (32) Bransfield Strait.

Figure DR3. Deposit densities in the neovolcanic zones versus spreading rate for the mid-ocean ridges. Deposit densities are represented by the distance between adjacent deposits or clusters of deposits more than 10 km apart (n = 70). Distances greater than 333 km (corresponding to the maximum L value of Baker, 2007) were considered to be out of range. The trendline fitted to the points shows that the spacing between deposits increases linearly with decreasing spreading rate, similar to predictions from heat flux models (Baker, 2007).

Figure DR4. Cumulative frequency plot of the sizes of seafloor massive sulfide (SMS) deposits. The plotted data are binned tonnages for 62 of the best mapped deposits (modified after Hannington et al., 2010; see **Table DR1**). The size classes were estimated using the area versus tonnage relationships for a number of drilled deposits as a guide and are plotted at the midpoints of each bin. Only those deposits having surface areas larger than 100 m^2 (~3,000 tonnes, n=42),

accounting for 67% of the population, are included on the plot. The deposits in the largest size class (top 10%) include Middle Valley, Zenith-Victory, Puys des Folles (~10 x 10^6 t), Semyenov (~9 x 10^6 t), Krasnov (~3 x 10^6 t), Sunrise (~3 x 10^6 t), the TAG Mound (2.7 x 10^6 t), and Solwara 1 (2.1 x 10^6 t). The deposits in the Atlantis II Deep of the Red Sea are excluded. The plot defines a general tonnage curve (power-law distribution); the intercept for the 50^{th} percentile indicates a median deposit size of 70,000 tonnes. No distinction is made between deposits on the mid-ocean ridges and deposits in arc and back-arc settings. So far, no deposits have been found in back-arc basins or on active volcanic arcs that are significantly larger than those on mid-ocean ridges. Therefore, a separate tonnage model for subduction-related environments is not justified at this time.

Table DR1. Summary data, including estimated deposit sizes, for a subset of seafloor massive sulfide deposits located in **Figure DR1**. Numbers refer to map locations. The data were compiled from Hannington et al. (2002, 2004), updated by Hannington et al. (2005), Hannington and Monecke (2009) and Beaulieu (2010). Area estimates are indicated only for those deposits for which published maps or other detailed descriptions are included in the literature or in the global database. Numbers represent cumulative area of exposed sulfide where multiple vent complexes or mounds are included as part of one deposit.

Table DR2. Summary data on the occurrence of seafloor massive sulfide deposits in 32 control areas used to measure deposit densities. The permissive areas listed in the table are assumed to extend no more than 50 km on either side of the spreading ridge or arc. The numbers of deposits include all 129 occurrences in the control areas. The spacing between deposits is based on 106 occurrences with reported dimensions of more than 100 m^2 on the seafloor as the minimum unit and clusters of mounds or vent complexes spatially separated from the next nearest cluster by more than 10 km. The locations of the control areas are indicated in **Figure DR2**.

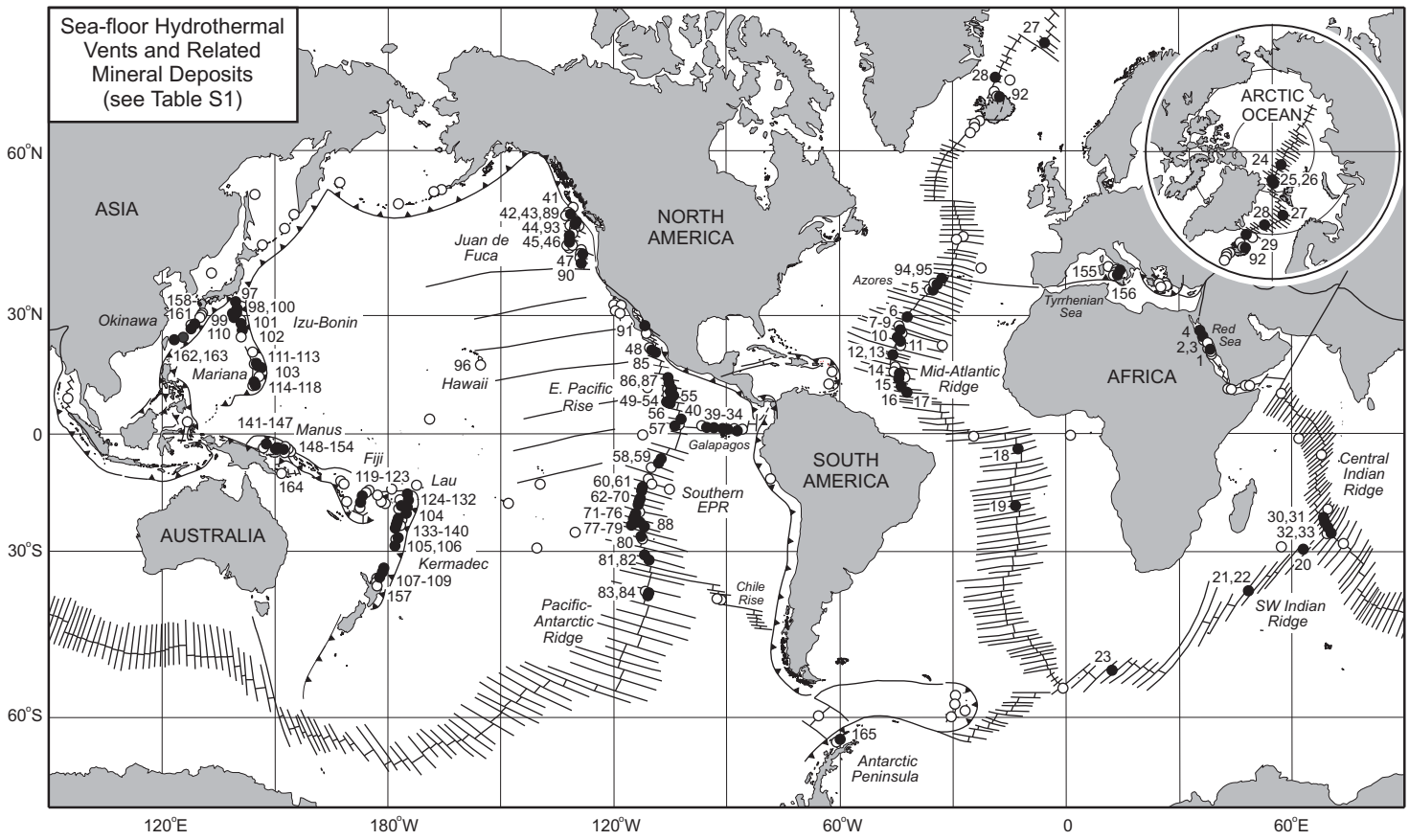
Sea-floor Hydrothermal Vents and Related Mineral Deposits (see Table S1)
ASIA
NORTH AMERICA
SOUTH AMERICA
AFRICA
AUSTRALIA
ARCTIC OCEAN
Juan de Fuca
Hawaii
E. Pacific Rise
Galapagos
Southern EPR
Chile Rise
Pacific-Antarctic Ridge
Okinawa
Izu-Bonin
Mariana
Manus
Fiji
Lau
Kermadec
Azores
Mid-Atlantic Ridge
Tyrrhenian Sea
Red Sea
Central Indian Ridge
SW Indian Ridge
Antarctic Peninsula
60°N
30°N
0
30°S
60°S
120°E
180°W
120°W
60°W
0
60°E

Figure DR1

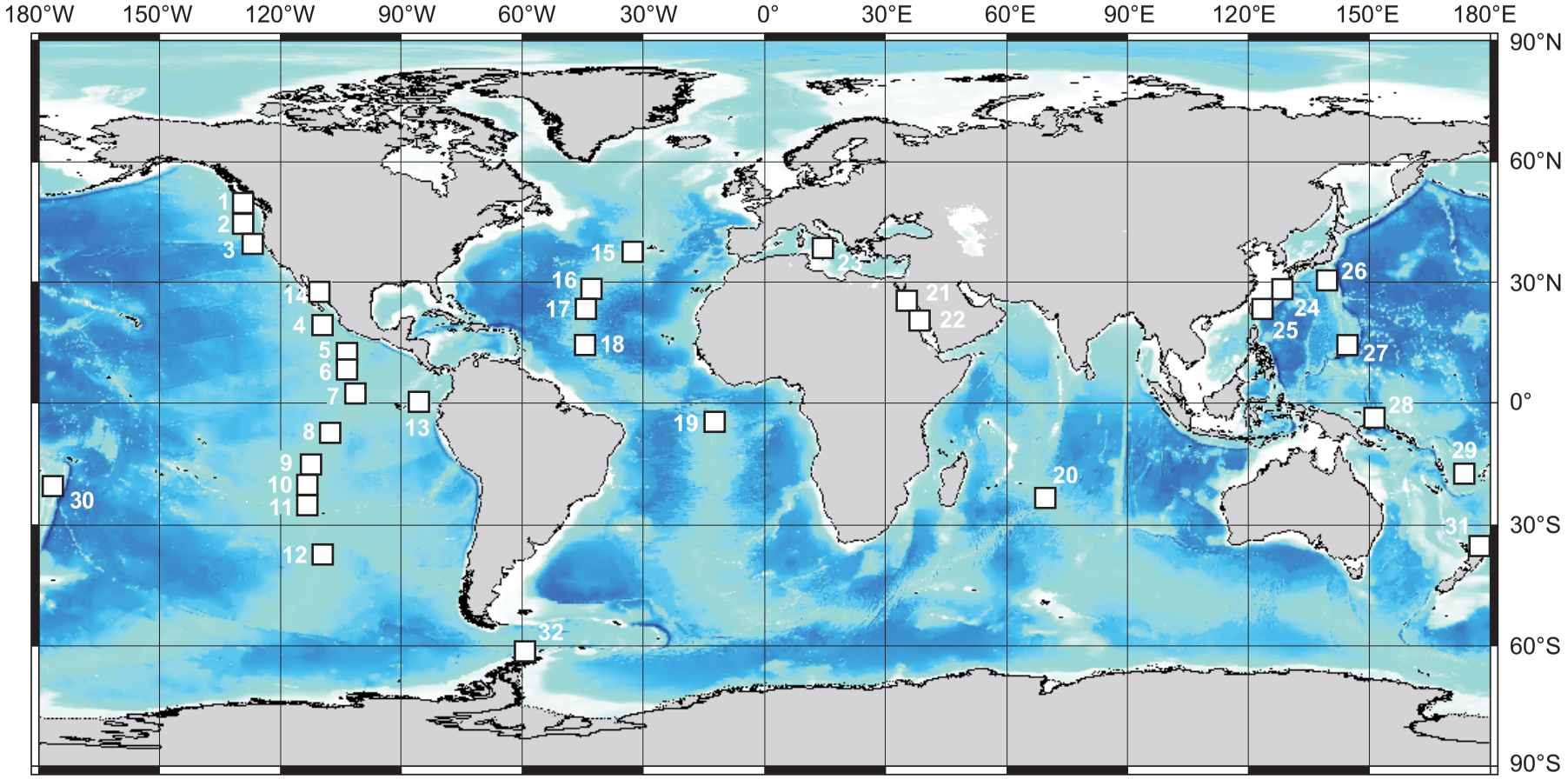

Equidistant Cylindrical Projection
Data: GEBCO Digital Atlas

Figure DR2

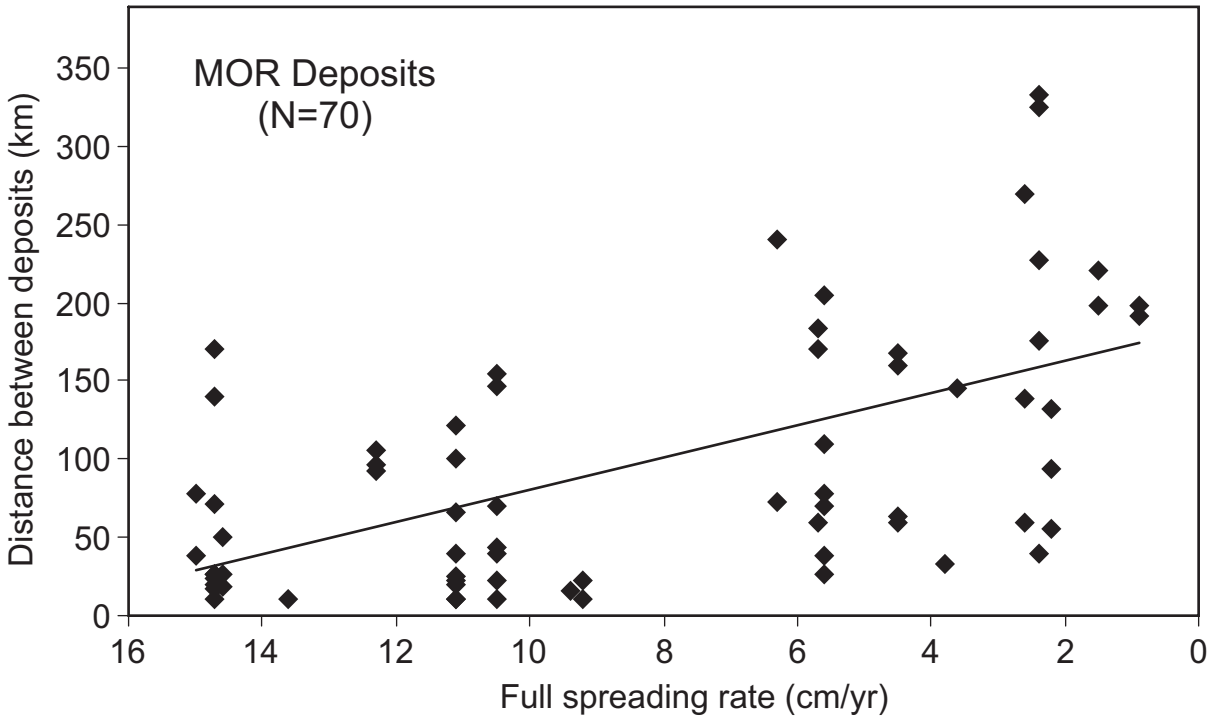
MOR Deposits
(N=70)
Distance between deposits (km)
350
300
250
200
150
100
50
0
16
14
12
10
8
6
4
2
0
Full spreading rate (cm/yr)

Figure DR3

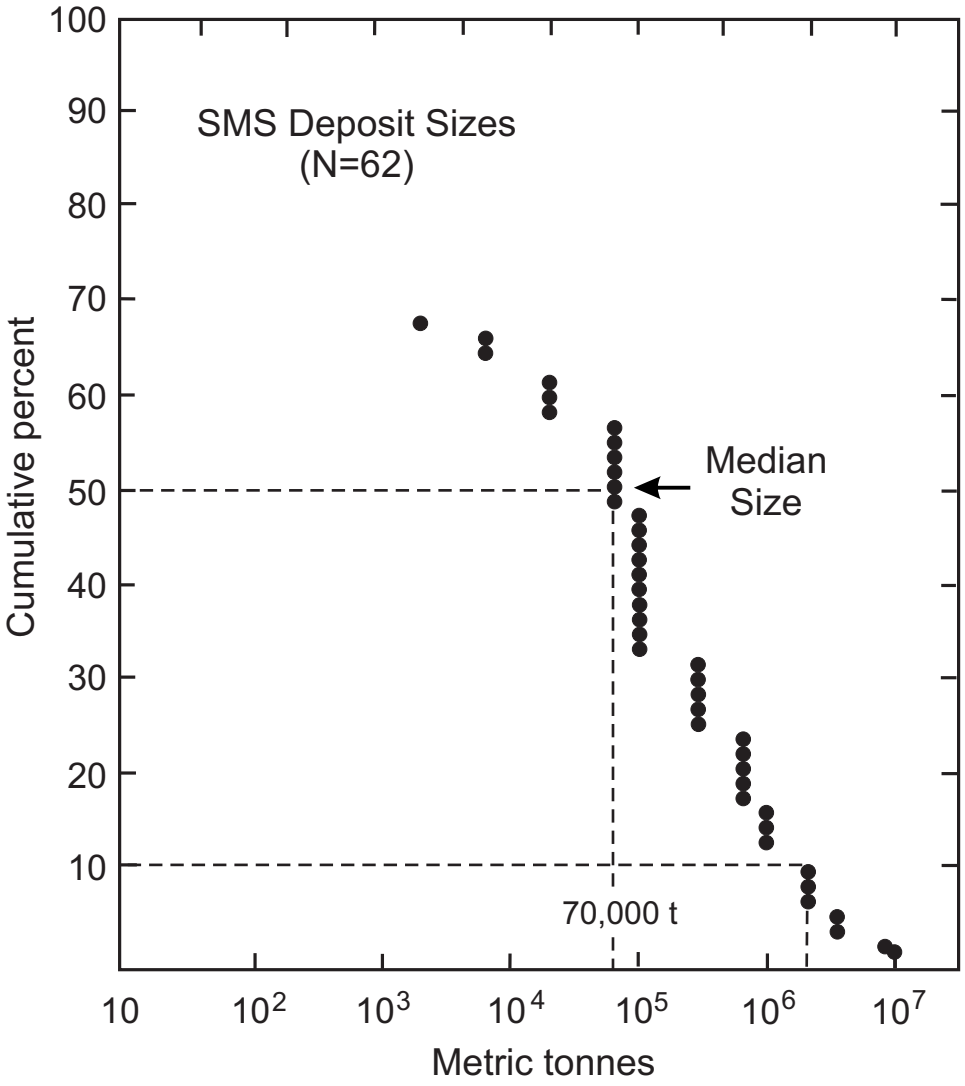
SMS Deposit Sizes
(N=62)
Median
Size
70,000 t
Cumulative percent
Metric tonnes
100
90
80
70
60
50
40
30
20
10
10
10^2
10^3
10^4
10^5
10^6
10^7

Figure DR4

Table DR1. Summary Data of Seafloor Massive Sulfide Deposits at 165 Sites (Figure DR1).

Map Location	Site	Full Spreading Ra (cm/yr)	Setting	Activity	Outcrop Area (m^2)	Estimated Size Range (tonnes)
Intracontinental rifts:						
1	Atlantis II Deep, Red Sea	1.5	Brine Pool	Active	--	90,000,000
2	Thetis, Nereus, Gypsum Deeps	1.0-1.5	Brine Pool	Active	--	--
3	Kebrit Deep, Red Sea	0.9	Brine Pool	Active	--	--
4	Shaban Deep, Red Sea	<0.8	Brine Pool	Active	--	--
Slow-spreading mid-ocean ridges:						
5	Rainbow Field, Mid-Atlantic Ridge	2.1	Ultramafic	Active	30,000	300,000-1,000,000
6	Broken Spur, Mid-Atlantic Ridge	2.3	MORB	Active	5,000	100,000-300,000
7	TAG Mound, Mid-Atlantic Ridge	2.4	MORB	Active/Inactive	30,000	2,700,000†
8	MIR Zone, Mid-Atlantic Ridge	2.4	MORB	Inactive	>50,000	1,000,000-3,000,000
9	Alvin Zone, Mid-Atlantic Ridge	2.4	MORB	Inactive	100,000	2,000,000
10	24°30'N, Mid-Atlantic Ridge	2.4	MORB	Active/Inactive	--	--
11	Snakepit Field, Mid-Atlantic Ridge	2.4	MORB	Active	15,000	100,000-300,000
12	Puy des Folles, Mid-Atlantic Ridge	2.6	MORB	Inactive	--	--
13	Zenith-Victory, Mid-Atlantic Ridge	2.6	MORB	Inactive	--	10,000,000
14	Krasnov, Mid-Atlantic Ridge	2.6	MORB	Active/Inactive	150,000	>3,000,000
15a	Logatchev 1, Mid-Atlantic Ridge	2.6	Ultramafic	Active/Inactive	>5,000	100,000-300,000
15b	Logatchev 2, Mid-Atlantic Ridge	2.6	Ultramafic	Active/Inactive	1,000	10,000-30,000
16	13°30'N Semyenov, Mid-Atlantic Ridge	2.6	MORB	Inactive	>300,000	9,000,000
17a	Ashadze 1, Mid-Atlantic Ridge	2.6	Ultramafic	Active/Inactive	>50,000	1,000,000-3,000,000
17b	Ashadze 2, Mid-Atlantic Ridge	2.6	Ultramafic	Active/Inactive	>50,000	1,000,000-3,000,000
18	5°S, Turtle Pits, Mid-Atlantic Ridge	3.6	MORB	Active	5,000	100,000-300,000
19	8°18'S, Nibelungen, Mid-Atlantic Ridge	3.6	MORB	Active	--	--
20	Mt. Jourdanne, Southwest Indian Ridge	1.4	MORB/Ultramafic	Inactive	≤100	<3,000
21	Segment 28, Southwest Indian Ridge	1.4	MORB	Active	--	--
22	Segment 27, Southwest Indian Ridge	1.4	MORB	Inactive	--	--
23	13°E, Southwest Indian Ridge	1.4	MORB	Active/Inactive	--	--
24	Gakkel Ridge, Arctic Ocean	1.1	MORB/Ultramafic	Active/Inactive	--	--
25	Aurora Field, Arctic Ocean	1.3	MORB/Ultramafic	Active/Inactive	--	--
26	Lena Trough, Arctic Ocean	1.3	MORB/Ultramafic	Inactive	--	--
27	Mohns-Knipovich Ridge	<1.0	MORB	Active	--	--
28	Mohns Ridge	<1.0	MORB	Active	--	--
29	Northern Kolbeinsey Ridge	1.7	MORB	Inactive	--	--
Intermediate-rate mid-ocean ridges:						
30	JX/MESO Zone, Central Indian Ridge	4.5	MORB	Inactive	>50,000	1,000,000-3,000,000
31	EX/FX Zone, Central Indian Ridge	4.4	MORB	Active(?)	--	--
32	Kairei Field, Central Indian Ridge	4.8	MORB	Active	3,000	30,000-100,000
33	Edmond Field, Central Indian Ridge	4.6	MORB	Active	3,000	30,000-100,000
34	Galapagos Rift, 86°W	6.3	MORB	Inactive	30,000	300,000-1,000,000
35	Galapogos Rift, 89°30'W	6.3	MORB	Active/Inactive	--	--
36	Galapogos Rift, 90°33'W	6.3	MORB	Active/Inactive	--	--
37	Galapogos Rift, Navidad	4.7-6.3	MORB	Active/Inactive	--	--
38	Galapogos Rift, Pinguinos, Iguanas	4.7-6.3	MORB	Active/Inactive	--	--
39	West Galapagos Rift, 91°50'W	4.7-6.3	MORB	Active/Inactive	--	--
40	West Galapagos Rift, 102°W	4.7-6.3	MORB	Inactive	--	--
41	Southern Explorer Ridge	5.7	MORB	Active/Inactive	5,000	100,000-300,000
42	High-Rise, Endeavour Ridge	5.7	MORB	Active	3,000	30,000-100,000
43a	Main Field, Endeavour Ridge	5.7	MORB	Active	5,000	100,000-300,000
43b	Clam Bed, Endeavour Ridge	5.7	MORB	Active	≤100	<3,000
43c	Mothra, Endeavour Ridge	5.7	MORB	Active	5,000	100,000-300,000
44	CoAxial Site, Juan de Fuca Ridge	5.6	MORB	Active	≤100	<3,000
45	North Cleft, Juan de Fuca Ridge	5.6	MORB	Active	≤100	<3,000
46	South Cleft, Juan de Fuca Ridge	5.6	MORB	Active	≤100	<3,000
47	North Gorda Ridge	5.6	MORB	Active	--	--
Fast-spreading mid-ocean ridges:						
48	9°45'N, EPR Flank	11.1	MORB	Active	--	--
49	10°20'N, EPR Flank	11.1	MORB	Active	--	--
50	21°N, Northern EPR	9.2	MORB	Active	≤100	<3,000
51	12°50'N, Northern EPR	10.5	MORB	Active	5,000	100,000-300,000
52	12°42'N, Northern EPR	10.5	MORB	Active	--	--

53	11°32'N, EPR Seamount	10.7	MORB	Inactive	≤100	<3,000
54	11°30'N, Northern EPR	10.7	MORB	Active	≤100	<3,000
55	11°N, Northern EPR	10.9	MORB	Active	≤100	<3,000
56	9-10°N, Northern EPR	11.1	MORB	Active	≤100	<3,000
57	1°44'N, AHA Field, EPR	12.3	MORB	Active	--	--
58	7°00'S, Southern EPR	13.6	MORB	Active	--	--
59	7°24'S, Southern EPR	13.7	MORB	Active	≤100	<3,000
60	14°00'S, Southern EPR	14.4	MORB	Active	--	--
61	15°00'S, Southern EPR	14.5	MORB	Active	--	--
62	16°43'S, Southern EPR	14.6	MORB	Active	≤100	<3,000
63	17°12'S, Southern EPR	14.6	MORB	Active	--	--
64	17°26'S, Southern EPR	14.6	MORB	Active	≤100	<3,000
65	17°27'S, Southern EPR	14.6	MORB	Active	--	--
66	17°34'S, Southern EPR	14.6	MORB	Active	--	--
67	18°00'S, Southern EPR	14.7	MORB	Active	--	--
68	18°11'S, Southern EPR	14.7	MORB	Active	--	--
69	18°26'S, Southern EPR	14.7	MORB	Active	≤100	<3,000
70	18°36'S, Southern EPR	14.7	MORB	Active	--	--
71	20°00'S, Southern EPR	14.6	MORB	Active	--	--
72	20°40'S, Southern EPR	14.8	MORB	Active	--	--
73	20°50'S, Southern EPR	14.8	MORB	Active	--	--
74	21°25'S, Southern EPR	14.9	MORB	Active	--	--
75	21°33'S, Southern EPR	14.9	MORB	Active	≤100	<3,000
76	21°50'S, Southern EPR	14.9	MORB	Active	≤100	<3,000
77	22°30'S, Southern EPR	14.9	MORB	Active	--	--
78	23°32'S, Easter Microplate	14.9	MORB	Active	--	--
79	23°50'S, Easter Microplate	15	MORB	Active	--	--
80	26°12'S, Easter Microplate	15	MORB	Active	--	--
81	31°09'S, Southern EPR	9.4	MORB	Active	--	--
82	31°51'S, Southern EPR	9.4	MORB	Active	--	--
83	37°40'S, Pacific-Antarctic Ridge	9.4	MORB	Active	≤100	<3,000
84	37°48'S, Pacific-Antarctic Ridge	9.4	MORB	Active	--	--
Off-axis volcanoes:						
85	Green Seamount	9.2	MORB Seamount	Inactive	300	3,000-10,000
86	14°N, Northern EPR	10.3	MORB Seamount	Inactive	≤100	<3,000
87	13°N, Northern EPR	10.5	MORB Seamount	Inactive	30,000	300,000-1,000,000
88	23°19'S, Pito Seamount	14.9	MORB	Active	--	--
Sedimented ridges and related rifts:						
89	Middle Valley (Bent Hill, ODP Mound)	5.4	Sedimented Rift	Active/Inactive	>50,000	10,000,000†
90	Escanaba Trough	2.4	Sedimented Rift	Active	1,000	10,000-30,000
91	Guaymas Basin	3.8	Sedimented Rift	Active	15,000	100,000-300,000
92	Grimsey Hydrothermal Field	1.8	Sedimented Rift	Active	--	--
Ridge-hotspot intersections:						
93	Axial Seamount, Juan de Fuca Ridge	5.6	MORB Seamount	Active	≤100	<3,000
94	Lucky Strike, Azores	2.2	MORB Seamount	Active	3,000	30,000-100,000
95	Menez Gwen, Azores	2	MORB Seamount	Active	--	--
Intraplate volcano:						
96	Loihi Seamount, Hawaii	na	OIB Seamount	Active	--	--
Intraoceanic arcs:						
97	Sunrise Deposit, Izu-Bonin Arc	na	Arc volcano	Active	150,000	>3,000,000
98	Kita Bayonnaise, Izu-Bonin Arc	na	Arc volcano	Active	--	--
99	Hakurei Deposit, Izu-Bonin Arc	na	Arc volcano	Active	--	--
100	Myojinsho, Izu-Bonin Arc	na	Arc volcano	Active/Inactive	--	--
101	Suiyo Seamount, Izu-Bonin Arc	na	Arc volcano	Active	3,000	30,000-100,000
102	Kaikata Seamount, Izu-Bonin Arc	na	Arc volcano	Active/Inactive	--	--
103	East Diamante, Mariana Arc	na	Arc volcano	Active	--	--
104	Volcano 1, Tonga-Tofua Arc	na	Arc volcano	Active	--	--
105	Volcano 19, Tonga-Tofua Arc	na	Arc volcano	Active	--	--
106	Monowai Caldera, Kermadec Arc	na	Arc volcano	Active/Inactive	--	--
107	Clark Seamount, Kermadec Arc	na	Arc volcano	Inactive	--	--
108	Rumble II West, Kermadec Arc	na	Arc volcano	Active	--	--
109	Brothers, Kermadec Arc	na	Arc volcano	Active	5,000	100,000-300,000
Intraoceanic back-arc basins:						
110	Sumisu Rift, Izu-Bonin Arc	na	Back-arc Basin	Active/Inactive	--	--
111	Alice Springs, Mariana Trough	2.6	Back-arc Basin	Active	1,000	10,000-30,000
112	18°13'N, Central Mariana Trough	2.6	Back-arc Basin	Active	--	--
113	18°02'N, Central Mariana Trough	2.6	Back-arc Basin	Active	--	--

114	13^{o}N, Southern Mariana Trough	3.5	Back-arc Basin	Active	300	3,000-10,000
115	Forecast Field, Southern Mariana Arc	3.5	Back-arc Basin	Active	--	--
116	Fryer Site, Southern Mariana Arc	3.5	Back-arc Basin	Active	--	--
117	Archean Seamount, Southern Mariana	3.5	Back-arc Basin	Active	--	--
118	Pika Seamount, Southern Mariana Arc	3.5	Back-arc Basin	Active	--	--
119	Sonne99 Corner Mound, North Fiji Basin	7	Back-arc Basin	Active	5,000	100,000-300,000
120	Sonne99 Yogi Mound, North Fiji Basin	7	Back-arc Basin	Active	--	--
121	Kaiyo Field, North Fiji Basin	7	Back-arc Basin	Active	--	--
122	White Lady, North Fiji Basin	7	Back-arc Basin	Active	--	--
123	Pere Lachaise, North Fiji Basin	7	Back-arc Basin	Active	5,000	100,000-300,000
124	Papatua Site, Northern Lau Basin	8.5	Back-arc Basin	Active(?)	--	--
125	Kings Triple Junction, Northern Lau	8.5	Back-arc Basin	Inactive	--	--
126	MTJ Caldera, Mangatolo Triple Junction	na	Back-arc Basin	Active/Inactive	--	--
127	Northeast Lau Spreading Center	9.4	Back-arc Basin	Active/Inactive	--	--
128	Maka Volcano, Northeast Lau Basin	na	Back-arc Basin	Active/Inactive	--	--
129	Plume Site, Northeast Lau Basin	9.4	Back-arc Basin	Active	--	--
130	Niua Site, Northeast Lau Basin	9.4	Back-arc Basin	Active	--	--
131	Fonualei Rift, Northeast Lau Basin	4.7-8.5	Back-arc Basin	Active	--	--
132	Central Lau Basin	4	Back-arc Basin	Active/Inactive	--	--
133	Kilo Moana, Southern Lau Basin	6	Back-arc Basin	Active	--	--
134	Tow Cam Field, Southern Lau Basin	6	Back-arc Basin	Active	--	--
135	ABE, CDE Fields, Southern Lau Basin	6	Back-arc Basin	Active	--	--
136	White Church, Southern Lau Basin	6	Back-arc Basin	Active	--	--
137	Tui Malila, Southern Lau Basin	6	Back-arc Basin	Active	--	--
138	Mariner, Southern Lau Basin	6	Back-arc Basin	Active	--	--
139	Vai Lili Field, Southern Lau Basin	6	Back-arc Basin	Active	--	--
140	Hine Hina, Southern Lau Basin	6	Back-arc Basin	Active/Inactive	--	--
141	Western Manus Basin (Solwara 11)	>5	Back-arc Basin	Active	--	--
142	Mata Na Taru, Western Manus Basin	>5	Back-arc Basin	Active	--	--
143	Central Manus Basin	>5	Back-arc Basin	Inactive	--	--
144	3^{o}22'S, Central Manus Basin	>5	Back-arc Basin	Active	--	--
145	Central Manus Basin (Solwara 10)	>5	Back-arc Basin	Active(?)	--	--
146	Vienna Woods (Solwara 2)	>5	Back-arc Basin	Active	--	--
147	Central Manus Basin (Solwara 3)	>5	Back-arc Basin	Active(?)	--	--
Transitional island arcs and back-arc rifts:						
148	Pacmanus, Eastern Manus (Solwara 4)	1.4	Back-arc Basin	Active/Inactive	15,000	100,000-300,000
149a	Solwara 6, Eastern Manus Basin	1.4	Back-arc Basin	Active(?)	15,000	100,000-300,000
149b	Solwara 7, Eastern Manus Basin	1.4	Back-arc Basin	Active(?)	15,000	100,000-300,000
149c	Solwara 8, Eastern Manus Basin	1.4	Back-arc Basin	Active(?)	--	--
150a	Desmos Cauldron, E. Manus Basin	1.4	Back-arc Basin	Active	--	--
150b	Solwara 12, Eastern Manus Basin	1.4	Back-arc Basin	Active(?)	--	--
151	Solwara 13, Eastern Manus Basin	1.4	Back-arc Basin	Active(?)	--	--
152	Solwara 1, Eastern Manus Basin	1.4	Back-arc Basin	Active	90,000	2,170,000†
153	Solwara 5, Eastern Manus Basin	1.4	Back-arc Basin	Active(?)	30,000	300,000-1,000,000
154	SuSu Knolls, Eastern Manus (Solwara 9)	1.4	Back-arc Basin	Active/Inactive	--	--
155	Palinuro Seamount, Tyrrhenian Sea	na	Arc volcano	Inactive	3,000	30,000-100,000
156	Panarea Seamount, Tyrrhenian Sea	na	Arc volcano	Active	--	--
157	Calypso Vents, Taupo Zone	na	Arc volcano	Active	--	--
Intracontinental back-arc rifts:						
158	Minami-Ensei, Okinawa Trough	2	Back-arc Basin	Active	--	--
159	North Iheya, Okinawa Trough	2	Back-arc Basin	Active	--	--
160	Clam Site, Okinawa Trough	2	Back-arc Basin	Active	--	--
161	Izena Cauldron, Okinawa Trough	2	Back-arc Basin	Active	5,000	100,000-300,000
162	Hatoma Knoll, S. Okinawa Trough	4	Back-arc Basin	Active	--	--
163	Yonaguni Knoll, S. Okinawa Trough	4	Back-arc Basin	Active	--	--
Volcanic rifted margins:						
164	Franklin Seamount, Woodlark Basin	2.7	Back-arc Basin	Inactive	--	--
165	Bransfield Strait, Antarctica	<1	Back-arc Basin	Inactive	--	--

Deposit sizes indicated with † are based on drilled/cored intersections. na = not applicable. "--" reliable information on size is not available. MORB= mid-ocean ridge basalt; OIB = ocean island basalt.

Table DR2. Deposit densities in 32 control areas (5° x 5°) containing 129 occurrences.

	Control Area (5 deg. x 5 deg.)	Full Spreading Rate (cm/yr)	Estimated Permissive Area (km^2)	Number of Occurrences in the Area (N=129)	Av. Spacing Between Deposits (km)
	Mid-Ocean Ridges:				
1.	N. Juan de Fuca Ridge	5.7	56,000	3	138
2.	S. Juan de Fuca Ridge	5.6	40,000	5	74
3.	Gorda Ridge	5.6	50,000	4	116
4.	EPR, 21°N	9.2	50,000	3	16
5.	EPR, 13°N	10.5	80,000	8	69
6.	EPR, 9°N	11.1	50,000	8	46
7.	EPR, 2°N	12.3	50,000	3	98
8.	EPR, 7°S	13.6	40,000	2	10
9.	EPR, 17°S	14.6	60,000	4	32
10.	EPR, 18°S	14.7	60,000	9	56
11.	Easter Microplate, 23°S	15.0	110,000	4	149
12.	Pacific-Antarctic Ridge, 37°S	9.4	50,000	2	16
13.	West Galapagos Rift, 91°W	6.3	50,000	3	156
14.	Guaymas Basin	3.8	40,000	2	33
15.	MAR, 37°N (Lucky Strike, Menez)	2.2	75,000	4	94
16.	MAR, 26°N (TAG, Broken Spur)	2.4	50,000	2†	>300
17.	MAR, 24°N and Snakepit	2.4	45,000	4	192
18.	MAR, 13°N and Logatchev	2.6	60,000	4	155
19.	MAR, 5°S	3.6	60,000	3	247
20.	Central Indian Ridge	4.5	50,000	5	113
21.	N. Red Sea	0.9	50,000	3	195
22.	S. Red Sea	1.5	52,000	2	209
	Arcs and Back-arc Basins:				
23.	Tyrrhenian Sea	--	35,000	3	75
24.	N. Okinawa Trough	2.0	60,000	4	53
25.	S. Okinawa Trough	4.9	45,000	3	114
26.	Izu-Bonin Arc	--	65,000	6	107
27.	Southern Mariana	--	75,000	5	100
28.	Eastern Manus Basin	1.4	25,000	6	63
29.	N. Fiji Basin	7.0	40,000	3	110
30.	S. Lau Basin	6.0	50,000	7	73
31.	Southern Kermadec Arc	--	70,000	3	104
32.	Bransfield Strait	--	40,000	2	100
	Average		**54,000**	**4.0**	**107**

Deposits considered in this study include only those occurrences that are larger than 100 m^2, thus eliminating the possibility of counting individual vents or small chimney complexes as "deposits". Permissive areas include seafloor up to 50 km from the ridge axis. Deposit spacings are averages of N deposits in each control area. Distances greater than 333 km (maximum L value of Baker, 2007) were considered to be out of range and not included in the data set. At the map scale chosen for this study, the TAG "deposit"† includes the TAG Mound, Alvin Zone and MIR Zone. The analyzed maps are provided as Supplementary Information.